

Prediction of liver cirrhosis, using diagnostic imaging tools

Suk Keu Yeom, Chang Hee Lee, Sang Hoon Cha, Cheol Min Park

Suk Keu Yeom, Sang Hoon Cha, Department of Radiology, Korea University Ansan Hospital, Korea University College of Medicine, Gyeonggi-do 425-707, South Korea

Chang Hee Lee, Cheol Min Park, Department of Radiology, Korea University Guro Hospital, Korea University College of Medicine, Seoul 152-703, South Korea

Author contributions: All the authors contributed to this work.

Conflict-of-interest statement: We disclose that authors have no conflict of interest about this manuscript.

Open-Access: This article is an open-access article which was selected by an in-house editor and fully peer-reviewed by external reviewers. It is distributed in accordance with the Creative Commons Attribution Non Commercial (CC BY-NC 4.0) license, which permits others to distribute, remix, adapt, build upon this work non-commercially, and license their derivative works on different terms, provided the original work is properly cited and the use is non-commercial. See: <http://creativecommons.org/licenses/by-nc/4.0/>

Correspondence to: Chang Hee Lee, MD, PhD, Department of Radiology, Korea University Guro Hospital, Korea University College of Medicine, 184, Gurodong-ro, Guro-gu, Seoul 152-703, South Korea. chlee86@korea.ac.kr
Telephone: +82-2-26263212
Fax: +82-2-8639282

Received: April 28, 2015

Peer-review started: May 6, 2015

First decision: June 25, 2015

Revised: July 15, 2015

Accepted: August 10, 2015

Article in press: August 11, 2015

Published online: August 18, 2015

Abstract

Early diagnosis of liver cirrhosis is important. Ultrasound-guided liver biopsy is the gold standard for diagnosis of liver cirrhosis. However, its invasiveness and sampling bias limit the applicability of the method. Basic imaging for the diagnosis of liver cirrhosis has developed over

the last few decades, enabling early detection of morphological changes of the liver by ultrasonography (US), computed tomography, and magnetic resonance imaging (MRI). They are also accurate diagnostic methods for advanced liver cirrhosis, for which early diagnosis is difficult. There are a number of ways to compensate for this difficulty, including texture analysis to more closely identify the homogeneity of hepatic parenchyma, elastography to measure the stiffness and elasticity of the liver, and perfusion studies to determine the blood flow volume, transit time, and velocity. Amongst these methods, elastography using US and MRI was found to be slightly easier, faster, and able to provide an accurate diagnosis. Early diagnosis of liver cirrhosis using MRI or US elastography is therefore a realistic alternative, but further research is still needed.

Key words: Liver fibrosis; Ultrasonography; Computed tomography; Magnetic resonance imaging; Magnetic resonance elastography; Sonoelastography; Acoustic radiation force impulse imaging

© **The Author(s) 2015.** Published by Baishideng Publishing Group Inc. All rights reserved.

Core tip: The development of new imaging modalities for liver cirrhosis has enabled early and accurate diagnosis of liver cirrhosis. Currently, elastography, used to measure the stiffness and elasticity of the liver, is more widely applied than texture. Ultrasound is simple imaging tool in diagnosing cirrhosis and can be added as several additional complementary technologies. The non-inferior diagnostic capability, non-invasiveness and relative cost-effectiveness of ultrasonography elastography may enable it to be one of the most useful techniques for diagnosis of liver cirrhosis.

Yeom SK, Lee CH, Cha SH, Park CM. Prediction of liver cirrhosis, using diagnostic imaging tools. *World J Hepatol* 2015; 7(17): 2069-2079 Available from: URL: <http://www.wjgnet.com/1948-5182/full/v7/i17/2069.htm> DOI: <http://dx.doi.org/10.4254/wjh.v7.i17.2069>

INTRODUCTION

Liver cirrhosis is the end stage of chronic liver disease. It is caused by diffuse fibrosis and regenerating nodules that result from recurrent necrosis of liver cell and degeneration. It is recognized as an irreversible form of parenchymal fibrosis. Liver cirrhosis reduces hepatic function and results in multiple complications induced by nodular regeneration and portal hypertension, including ascites, variceal bleeding, renal failure due to hepatorenal syndrome, hepatic encephalopathy, and spontaneous bacterial peritonitis. In addition, the incidence of hepatocellular carcinoma is sharply increased. Recently, early liver cirrhosis was shown to be improved by regression of collagen tissue^[1]. Regression is usually associated with the improvement of clinical status, but can vary in the degree of improvement, depending on the reversibility of liver damage. Extensive scarring with parenchymal destruction is unlikely to regress. Therefore, early diagnosis of liver cirrhosis and quantification of the proportion of fibrosis in the liver are very important in the management of chronic liver disease. Prognosis and management of chronic liver diseases hinge strongly on the amount and progression of liver fibrosis^[2,3].

There are a variety of causes of liver cirrhosis, with alcohol consumption, viruses, and fatty liver disease making up the majority of factors. These various etiologies induce chronic inflammation. Normal lobular architecture of the liver parenchyma is replaced by a parenchymal nodule surrounded by the fibrous tissue. Portal-central septa, connecting the portal vein and central vein, develop. As the inflammation persists, various form of fibrosis develops. The gross morphologic appearance of a cirrhotic liver is categorized by the size of the parenchymal nodules: micronodular, macronodular, or mixed. Micronodular cirrhosis is characterized by regenerative nodules of relatively uniform and small size. This pattern is seen in chronic alcoholic, hepatitis C, and biliary cirrhosis. In macronodular cirrhosis, the parenchymal nodules are larger, and more variable in size. Chronic hepatitis B is the most common cause of macronodular cirrhosis.

On the other hand, liver cirrhosis is classified according to the main location of fibrosis occurrence. A portal-based pattern usually results from hepatitis B and C, autoimmune hepatitis, Wilson's disease, primary biliary cirrhosis, primary sclerosing cholangitis, recurrent pyogenic cholangitis, and hemochromatosis. Conversely, a centrilobular fibrosis pattern results from alcoholic and nonalcoholic steatohepatitis or chronic venous outflow obstruction.

There are differences in the grading and scoring of fibrosis by microscopic pathology according to the cirrhosis pattern. The METAVIR score (F0: no fibrosis, F1: portal fibrosis without bridging fibrosis, F2: portal fibrosis with few bridging fibrosis, F3: bridging fibrosis with architectural distortion, F4: cirrhosis) and the Ishak score (grades four categories of activity/necrosis, 0-4 or 0-6) are commonly used systems for grading or

staging. The METAVIR score is simple, reproducible, and clinically validated, while the Ishak score is generally considered to be unnecessarily complex but preferred in many clinical trials^[4].

Pathological confirmation of microscopic specimens obtained by ultrasound-guided needle biopsy is the reference standard for fibrosis staging. However, there are several well-known limitations, including sampling errors, subjective interpretation, semiquantitativeness, invasiveness, morbidity, and mortality of the procedure^[5-7].

In clinical practice, the severity of liver cirrhosis is measured by multiple serologic biomarkers and many clinical scores and panels, such as the Child-Pugh score, model for end-stage liver disease score, FibroTest, HepaScore, FibroSpect, enhanced liver fibrosis score, and aspartate aminotransferase-to-platelet ratio index. However, these metrics also have many limitations, since the biomarkers are not liver-specific and measurement depends highly on their clearance and excretion^[8,9].

Basic imaging diagnosis of liver cirrhosis has developed over the last few decades, enabling early detection of morphological changes of the liver using ultrasonography (US), computed tomography (CT), and magnetic resonance imaging (MRI). These methods are accurate for diagnosis of advanced liver cirrhosis. However, as morphological changes indicate advanced cirrhosis, there are limitations to early diagnosis of liver cirrhosis using imaging. To facilitate early diagnosis of liver cirrhosis, texture analysis and elastography to measure stiffness of the liver, and perfusion studies to determine the blood flow volume, transit time, and velocity were developed.

In this review, we highlight the many efforts made to improve diagnostic accuracy of imaging modalities in early liver cirrhosis.

IMAGING MODALITIES

The classical role of many imaging modalities in liver cirrhosis diagnosis is the detection of morphological changes in the liver. Cirrhotic liver shows nodular hepatic contour, changes in volume distribution, including an enlarged caudate lobe and left lobe lateral segment, atrophy of the right and left lobe medial segments, widening of the fissures and the porta hepatis, and regenerative nodules (Figure 1). Secondary findings related to portal hypertension may present, including varices, ascites, splenomegaly, fatty infiltration in the omentum and mesentery, edematous wall thickening of gastrointestinal tracts due to venous congestion, and intrahepatic arterioportal or arteriovenous shunts (Figure 2).

However, there are limitations to the diagnosis of early fibrosis, because these morphologic changes of the liver and related secondary findings represent advanced liver cirrhosis.

US

Ultrasound is a safe and relatively inexpensive imaging

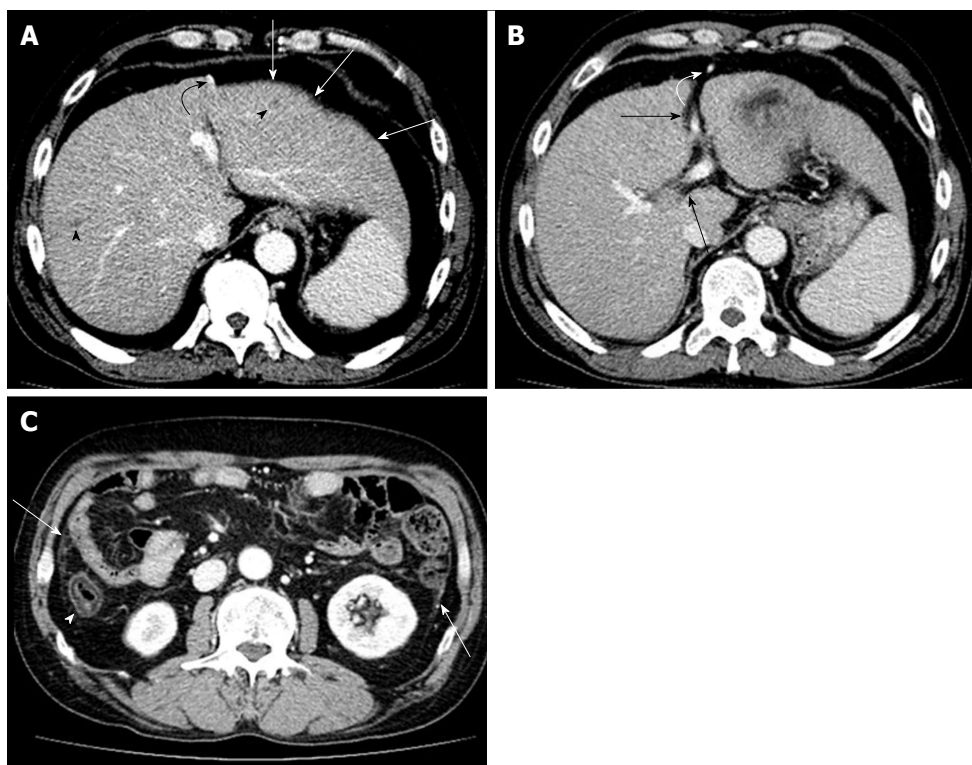


Figure 1 Contrast enhanced computed tomography portal phase images of the patient with liver cirrhosis due to chronic hepatitis B. A: Liver shows surface undulation (arrows). Two small low attenuated nodules are seen in both hepatic lobes suggesting regenerative nodules (arrow heads). Recanalized paraumbilical vein and paraesophageal varix are noted (curved arrow); B: Recanalization of paraumbilical vein (curved arrow) represents portal hypertension. Widening of hepatic fissure and porta hepatis is seen (black arrows); C: Ascending colon presents edematous wall thickening caused by congestion due to portal hypertension or hypoalbuminemic edema (curved arrow). Diffuse peritoneal thickening is also noted (arrows).

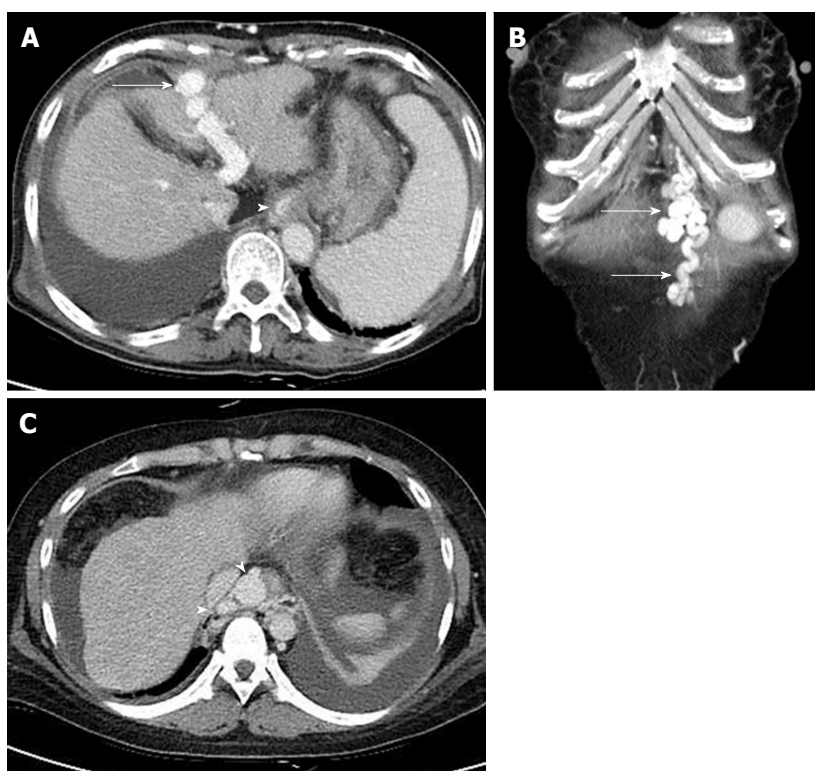


Figure 2 Image of liver cirrhosis caused by chronic hepatitis B. Contrast enhanced computed tomography portal phase images show multiple collateral vessels of portal vein. A: The image presents large intrahepatic portosystemic shunt through left portal vein and recanalized paraumbilical vein (arrow). Lower esophageal varix is seen (arrow head); B: Coronal image shows prominent paraumbilical veins (arrows); C: Axial image shows engorged paraesophageal varix (arrow heads) which usually supplied by left gastric vein and drained into azygos- or hemiazygos-vein.

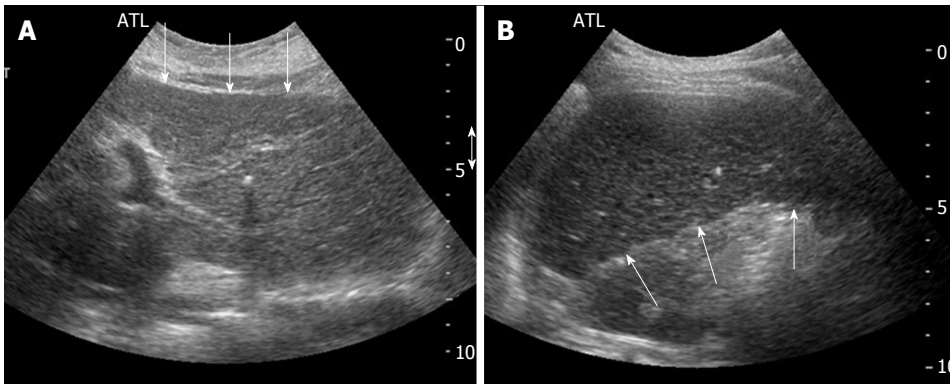


Figure 3 Transaxial scan. A: Transaxial epigastric scan shows the left lobe of the liver with surface irregularity (arrows), and coarse parenchyma echotexture; B: Subcostal transaxial scan shows the inferior margin of right hepatic lobe with irregular surface (arrows).

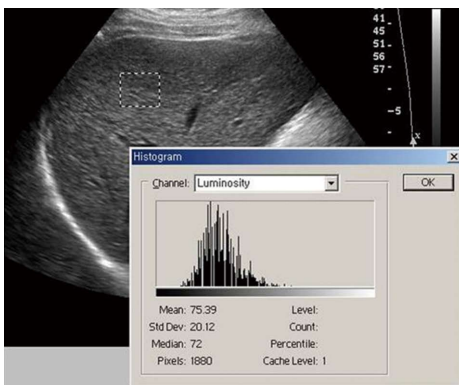


Figure 4 The region of interest of texture analysis is positioned in the right lobe of the liver, with an intercostals scan performed with gray scale ultrasonography. Chronic liver disease patient shows heterogeneous parenchymal echogenicity with high standard deviation value (Area: 1880 pixels, Mean: 75.39, SD: 20.12).

tool, allowing annual or biannual tests in chronic hepatitis patients. Initial findings of hepatic fibrosis by US are similar to simple hepatosteatosis^[10]. Fibrosis of the hepatic parenchyma attenuates beam penetration, increases parenchymal echogenicity, and decreases vascular conspicuity.

Liver cirrhosis is characterized by changes in liver volume distribution, surface nodularity, accentuation of the fissure, heterogeneity, bright and coarsening of the hepatic architecture, cirrhotic nodules including regenerative and dysplastic nodules, and signs of portal hypertension. Studies showed an overall sensitivity to chronic liver disease of 65%-95%, with a positive predictive value of 98%^[11-13]. The most indicative finding of liver cirrhosis was nodular surface, which was more sensitive on the undersurface of the liver than the superior surface (86% vs 53%) (Figure 3). It was also more sensitive in a high frequency probe^[11-13]. Although any single US feature had limited sensitivity or specificity in detecting cirrhosis, improvements could be achieved by combining two or three parameters.

US imaging can provide early detection of morphological changes of the liver, but such changes represent advanced cirrhosis. Furthermore, ultrasound

imaging is subjective and difficult to quantify, as inter- and intra-observer variability is a significant problem. There have been many efforts to objectively quantify the coarseness of hepatic parenchymal echogenicity. An initial study performed a simple quantification of parenchymal echogenicity and compared the standard deviation between chronic liver disease and normal liver (Figure 4)^[14-16]. The coarseness of hepatic parenchyma decreased beam penetration, while the attenuation of echogenicity according to depth increased proportionally to fibrosis. Methods that were more delicate were also introduced. Measurement of differences in echogenicity between neighboring pixels can be pathologically correlated to chronic liver disease^[17]. Texture analysis can improve diagnostic accuracy of grayscale US images. However, there are several limitations to the widespread use of these techniques, including dedicate post-processing programs, inter-observer variability, and sampling bias. The success of this approach also depends strongly on an expert to establish the regions of interest^[18].

In cirrhosis, Doppler waves of the hepatic vein show spectral broadening and hepatic vein narrowing. Phasic oscillations in hepatic venous flow are dampened. Normal phasicity of the hepatic vein represents a pressure change in the right atrium through the cardiac cycle. However, phasicity of the hepatic vein is reduced in liver cirrhosis, a result of decreased hepatic compliance and venous segments narrowed by adjacent regenerative nodules^[19]. The portal vein is initially dilated over 1.4 cm in diameter, but the emergence of the bypass collateral vessels changes hepatofugal blood flow and decreases the portal vein diameter to less than 1 cm. The hepatic artery has a high resistive index, but the development of a large arteriovenous shunt or arterioportal shunt leads to lower resistance^[20-22].

Development of contrast materials using micro-bubbles can help measure the blood transit time of the liver. Hepatic arterial/vein transit time decreases with fibrosis progression. It is known that intrahepatic arterioportal or arteriovenous shunt and arterializations of the cirrhotic liver leads to short blood transit times^[23,24]. However, these studies showed no significant

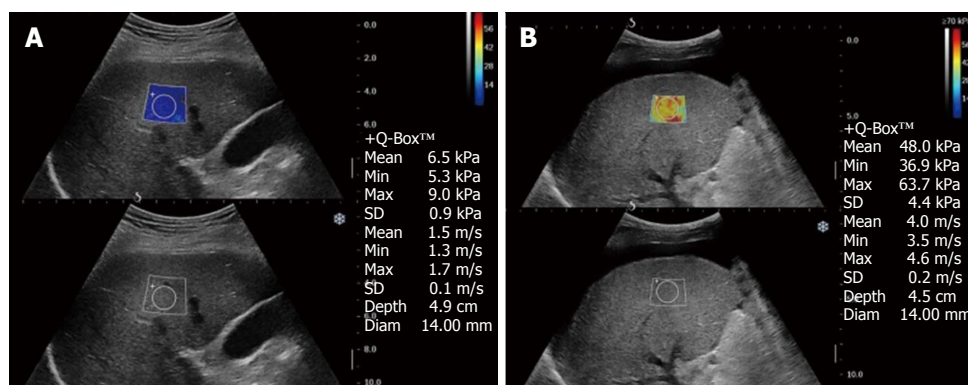


Figure 5 The region of interest of supersonic shear wave imaging is positioned in the right lobe of the liver, with an intercostals scan. On the right of the display there is shear wave velocity (expressed in kPa and m/s). The display show a real-time color mapping of the elasticity encoded pixel by pixel in an image superimposed on the standard B-mode. In panel (A) subject with normal shear wave speed value. In panel (B) patient with shear wave speed value compatible with liver cirrhosis. The display also shows large amount of ascites.

correlation between the severity of hepatic fibrosis and hemodynamic coefficients including hepatic vein transit time, hepatic artery transit time and intrahepatic transit time. The reason is that blood transit time is influenced by not only arteriportal or arteriovenous shunt, but also various extrahepatic and intrahepatic factors such as cardiac output and the degree of first-pass phagocytosis of contrast agent by Kupffer cells^[23].

US elastography is now widely recognized as a reliable method to assess liver fibrosis. The principle of elastography is the shearing of the examined tissue, which induces a smaller strain in hard tissues than in soft ones. There are several commercial types of US elastography currently in use: transient elastography (TE), acoustic radiation force impulse imaging (ARFI), Supersonic shear wave imaging (SSI), and real-time tissue elastography.

TE is performed with the Fibroscan™ (Echosens, Paris, France) which comprises of an ultrasound transducer probe located on the axis of a vibrator. The vibrator makes a vibration, which leads to an elastic shear wave propagating to the liver. The shear wave velocity (expressed in kiloPascals-kPa) is directly related to the stiffness of the tissue^[25]. At present, TE is the most widely used method for the liver fibrosis assessment. TE has been validated in various chronic liver diseases including chronic hepatitis B and C, nonalcoholic fatty liver disease^[26-29]. However, it has several limitations; the rate of unreliable measurements is reached up to 20% and the rate of reliable measurements decreased in obese patients and it cannot be performed in patients with ascites^[30].

ARFI technique is directly integrated on a standard US machine and shear wave is localized, allowing selection of the region of interest (ROI) by the operator on a real time US image. The ultrasound probe automatically produces an acoustic "push" pulse, generating shear-waves that propagate into the tissue. Transmission of a longitudinal acoustic pulse leads to tissue displacement, resulting in shear-wave propagation away from the region of excitation. Shear-wave velocity

(given in m/s) is measured within a defined ROI using US tracking beams laterally adjacent to the single push beam^[31]. Propagation speed increases with fibrosis severity. Results were similar to those with transient elastography^[29,32].

In contrast to TE and ARFI using a single shear wave emitted temporarily at a single frequency for each measurement, the ultrasound transducer of SSI technique (Aixplorer, Supersonic Imagine, Aix-en-Provence, France) emits a multiple pulse wave beams at increasing depths allowing the evaluation of the velocity of several shear wave fronts over a wide frequency range at the same time. By generating a real-time color mapping of the elasticity encoded pixel by pixel in an image superimposed on the standard B-mode, SSI allows to show the viscoelastic properties in all areas of an ROI with a color look-up table (Figure 5). This is expected to overcome the limitations of transient elastography, where liver stiffness cannot be measured accurately in patients with severe obesity, and ascites. Some articles have shown growing evidence for the accuracy of US elastography^[33-37] (Table 1). Although the low reproducibility of measurements derived from operator-dependent performance remains a significant limitation of US elastography, this technique is a useful diagnostic tool for hepatic fibrosis and further validation is warranted.

CT

CT is the most sensitive diagnostic tool for evaluating hepatic morphological changes^[38]. CT readily shows alterations in hepatic morphology and extra-hepatic manifestations related to portal hypertension. With liver cirrhosis progression, the nodularity of the liver surface and generalized heterogeneity of the hepatic parenchyma are visible. The porta hepatis and interlobar fissure frequently appear wider due to shrinkage of the right lobe and the medial segment of the left lobe with concomitant enlargement of the caudate lobe and the lateral segment of the left lobe. Changes in size and volume distribution are easily visible in a CT

Table 1 Diagnostic performance of ultrasonography elastography for hepatic fibrosis

Ref.	Year	Study method	Imaging instrument	Etiologies	No. of patients	Sensitivity (%)	Specificity (%)	Cut-offs	AUROC	Fibrosis score
Tada <i>et al</i> ^[33]	2015	Prospective	SSI	HCV	55	88.9	91.9	8.8 kPa	0.94	F2-3 (F4, excluded)
Samir <i>et al</i> ^[34]	2015	Prospective	SSI	Chronic viral and nonviral hepatopathies	136	91.4	52.5	7.29 kPa	0.84	≥ F2
Deffieux <i>et al</i> ^[63]	2015	Prospective	SSI	Chronic viral and nonviral hepatopathies	120	77	79	8.9 kPa	0.81	≥ F2
Yoon <i>et al</i> ^[35]	2014	Prospective	SSI	Chronic viral and nonviral hepatopathies	94	78.8	75.6	6.65 kPa	0.852	≥ F2
Tutar <i>et al</i> ^[36]	2014	Prospective	SSI	Children, viral and nonviral hepatopathies	76	97.8	96	10.4 kPa	0.96	≥ F2
Jeong <i>et al</i> ^[64]	2014	Prospective	SSI	Chronic viral and nonviral hepatopathies	70	78.2	93.3	8.6 kPa	0.915	≥ F2
Cassinotto <i>et al</i> ^[37]	2014	Prospective	SSI	Chronic viral and nonviral hepatopathies	336	83	82	8 kPa	0.89	≥ F2
			ARFI	Chronic viral and nonviral hepatopathies	341	72	81	1.38 m/s	0.81	≥ F2
			TE	Chronic viral and nonviral hepatopathies	337	76	81	8.5 kPa	0.83	≥ F2
Yap <i>et al</i> ^[31]	2013	Prospective	ARFI	Chronic viral and nonviral hepatopathies	70	68	66	1.55 m/s	0.85	≥ F2
Bota <i>et al</i> ^[32]	2013	Meta-analysis	ARFI	Chronic viral and nonviral hepatopathies	1163	74	83	1.30 m/s	0.85	≥ F2
			TE	Chronic viral and nonviral hepatopathies	1163	78	84	N/A	0.87	≥ F2
Ferraioli <i>et al</i> ^[65]	2012	Prospective	SSI	HCV	121	90	87.5	7.1 kPa	0.92	≥ F2
Chon <i>et al</i> ^[29]	2012	Meta-analysis	TE	HBV	2772	74.3	78.3	7.9 kPa	0.859	≥ F2
Friedrich-Rust <i>et al</i> ^[26]	2008	Meta-analysis	TE	Chronic viral and nonviral hepatopathies	8433	N/A	N/A	7.65 kPa	0.84	≥ F2

AUROC: Area under receiver operating characteristic; SSI: Supersonic shear wave imaging; HCV: Hepatitis C virus; ARFI: Acoustic radiation force impulse imaging; TE: Transient elastography (FibroScan™); HBV: Hepatitis B virus; N/A: Not applicable.

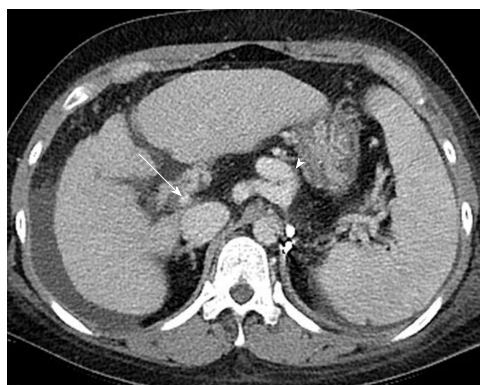


Figure 6 Image of liver cirrhosis caused by chronic hepatitis B. Contrast enhanced computed tomography portal phase image shows the liver with irregular surface and heterogeneous enhancement of parenchyma with reticular pattern suggesting confluent fibrosis. The image shows decreased diameter of portal vein (arrow) due to large collateral vessels (arrow head) and also shows large amount of ascites.

scan. In early stages, the liver may appear normal. The limited spatial resolution of CT and MRI allow detection of only a relatively thick fibrous septum. Thick fibrous septa and confluent hepatic fibrosis showed low attenuation in non-enhanced CT. The boundary between fibrosis and normal parenchyma was more ambiguous in a contrast-enhanced scan (Figure 6). Therefore, it is difficult to perform texture analysis

using CT. Considering the fact that the CT contrast agent is an extracellular space contrast agent, texture analysis is a method of measuring the decrease of the extracellular space fraction. When liver cirrhosis progress is enforced experimentally, there is a high correlation with the fibrosis grade, though this has not been proven clinically^[39].

Perfusion imaging in liver fibrosis is based on the occurrence of substantial microcirculatory changes in this disease. These changes are caused by capillarization of the sinusoids, collagen deposits in the extracellular space of Disse, and contraction of activated stellate cells^[40]. Quantification of hepatic perfusion by dynamic CT has allowed separate evaluations of arterial and portal perfusion of the liver^[41,42]. Perfusion CT can be used to detect microcirculatory changes that occur in cirrhosis and help to differentiate low-grade fibrosis^[43]. Perfusion CT had several limitations. It suffered from the classic CT limitations: radiation, the use of iodinated contrast agents and limited scan coverage range^[43]. However, new technological developments have reduced the scanning time and increased the detector size, enabling a reduction in the dose of radiation and expanding the scanning range.

MRI

MRI has several advantages over other imaging tech-

Table 2 Diagnostic performance of magnetic resonance elastography for hepatic fibrosis

Ref.	Year	Study method	Imaging instrument	Etiologies	No. of patients	Sensitivity (%)	Specificity (%)	Cut-offs	AUROC	Fibrosis score
Singh <i>et al</i> ^[66]	2015	Meta-analysis	1.5 Tesla, variable	Chronic viral and nonviralhepatopathies	697	79	81	3.66 kPa	0.88	≥ F2
Venkatesh <i>et al</i> ^[67]	2015	Retrospective	1.5 Tesla, (GE, Signa)	Chronic viral and nonviralhepatopathies	62	100	96.5	3.37 kPa	0.99	≥ F2
Yoon <i>et al</i> ^[56]	2014	Prospective	1.5 Tesla (GE, SignaHDx)	Chronic viral and nonviralhepatopathies	94	78.8	75.6	6.65 kPa	0.852	≥ F2
Venkatesh <i>et al</i> ^[68]	2014	Prospective	1.5 Tesla (GE, Signa)	HBV	63	97.4	100	3.2 kPa	0.99	≥ F2
Shi <i>et al</i> ^[69]	2014	Prospective	3.0 Tesla (GE, Signa Excite HD)	HBV	113	95	94.5	4.07 kPa	0.986	≥ F2
Loomba <i>et al</i> ^[70]	2014	Prospective	3.0 Tesla (GE, Signa Excite HD)	Nonalcoholic fatty liver disease	117	86	91	3.63 kPa	0.924	≥ F3
Bohte <i>et al</i> ^[71]	2014	Prospective	3.0 Tesla (Philips, Intera)	HBV, HCV	103	62	96	2.18 kPa	0.928	≥ F2
Kim <i>et al</i> ^[72]	2013	Retrospective	1.5 Tesla (GE, Signa)	Nonalcoholic fatty liver disease	142	85	92.9	4.15 kPa	0.954	≥ F3
Wang <i>et al</i> ^[73]	2012	Meta-analysis	1.5 Tesla, variable	Chronic viral and nonviralhepatopathies	972	94	95	N/A	0.98	≥ F2
Rustogi <i>et al</i> ^[54]	2012	Retrospective	1.5 Tesla (Siemens, Magnetom)	Chronic viral and nonviralhepatopathies	72	85.4	88.4	5.9 kPa	N/A	≥ F3
Kim <i>et al</i> ^[74]	2011	Prospective	1.5 Tesla (GE, SignaHDx)	Chronic viral and nonviralhepatopathies	55	89.7	87.1	3.05 kPa	N/A	≥ F2

AUROC: Area under receiver operating characteristic; HBV: Hepatitis B virus; HCV: Hepatitis C virus; N/A: Not applicable.

niques, including high-resolution images with excellent contrast against other soft tissue lesions and a number of different techniques facilitating the diagnostic evaluation of organ morphology, physiology, and function. As it is dependent on the detection of alterations in hepatic morphology, conventional MRI is limited to the diagnosis of earlier stages of liver fibrosis and is not suitable for disease staging^[44].

Calculation of the apparent diffusion coefficient (ADC) with diffusion-weighted imaging (DWI) using MRI can facilitate the assessment of liver fibrosis^[45]. One recent study showed that ADC values decrease with increasing stage of liver fibrosis from F0 to F4. However, no significant differences in ADC values were detected between the early stages of fibrosis^[46,47].

Intravoxel incoherent motion (IVIM)-DWI was developed to quantitatively assess the microscopic translational motions of both intracellular and extracellular water molecules occurring in each voxel in MRI. Using IVIM imaging, several factors, such as pure molecular diffusion and microcirculation or blood perfusion, can be distinguished with multiple *b* values^[48]. One study demonstrated that both ADC and perfusion-related diffusion (*D*^{*}) were significantly reduced in the cirrhotic liver group compared with those in the healthy liver group, while there was no significant difference between pure molecular-based diffusion (*D*) and perfusion fraction (*f*) measurements in the healthy liver and cirrhotic liver groups^[49]. ADC and *D*^{*} reduction in cirrhosis represents reduced perfusion in cirrhotic liver. Another study showed the feasibility of IVIM parameters in differentiating early stages of fibrosis^[50].

Magnetic resonance elastography (MRE) is an emerging technique that noninvasively quantifies liver

stiffness by analyzing the propagation of mechanical waves through liver tissue. It is based on the concept that the stiffness of the hepatic parenchyma is increased as fibrosis advances. One study showed that MRE has a high sensitivity and specificity in detecting liver fibrosis, with a predicted sensitivity and specificity of 91% and 97% for liver fibrosis ≥ stage F2, respectively; 92% and 95% for liver fibrosis ≥ stage F3, respectively; and 95% and 87% for liver fibrosis ≥ stage F4, respectively^[51]. Another study showed a sensitivity and specificity of 98% and 99% for all grades of liver fibrosis with a cut-off value of liver stiffness of 2.93 kPa^[52]. This study also showed that MRE could discriminate patients with moderate and severe fibrosis (grades 2-4) from those with mild fibrosis (sensitivity, 86%; specificity, 85%). Several studies show that MRE is more reliable for staging hepatic fibrosis compared to DWI and conventional MRI, with a powerful combination of sensitivity, specificity, likelihood ratios, diagnostic odds ratio, and area under the summary receiver operating characteristic curve values^[51,53-55] (Table 2). MRE can be easily added to standard abdominal MRI protocols, promising value added in staging liver cirrhosis. One study showed that MRE and SSI results moderately correlated with liver cirrhosis values, though MRE measurements tended to be more reliable than US elastography^[56].

MRE has many advantages: (1) it can exam the whole liver, with a lower sampling error than with a biopsy or other imaging modalities; (2) good diagnostic accuracy; and (3) the results are not influenced by hepatic steatosis, obesity, and ascites. However, some clinical limitations include: (1) misinterpretation of results due to a high iron overload in the liver, causing signal-

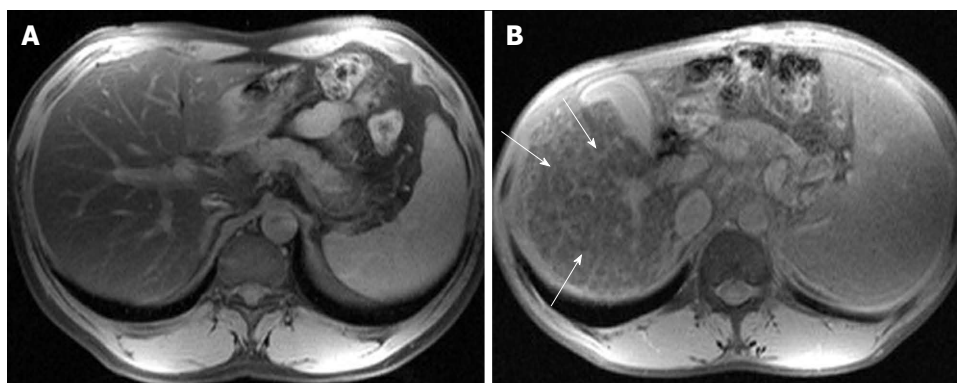


Figure 7 Double contrast enhanced protocol magnetic resonance images. Fat saturated T2-weighted magnetic resonance images of 15-min delay after injection of superparamagnetic iron oxides and gadolinium chelates. A: The image of normal patient shows homogenous low signal intensity of hepatic parenchyma; B: The image of patient with liver cirrhosis shows hyperintense reticulations (arrows), represent septal fibrosis, in cirrhotic liver.

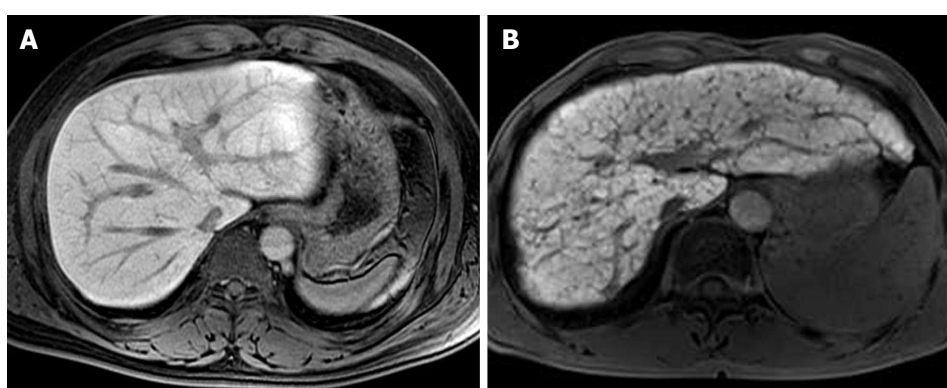


Figure 8 Fat saturated T1-weighted magnetic resonance images of 20-min delay after injection of gadoxetate disodium. A: The image of healthy patient shows homogenous high signal intensity of hepatic parenchyma; B: The image of patient with liver cirrhosis shows heterogeneity of hepatic parenchyma enhancement with hypointense reticulations representing septal fibrosis, and decreased enhancement degree as compared with the image (A).

to-noise limitations; (2) a longer examination time than SSI; (3) the need for dedicated installation equipment; and (4) a lack of comparable studies between 1.5 Tesla and 3.0 Tesla MRI machines and among other company products (Table 2). Therefore, an absolute cut-off value for diagnosis and grading of hepatic fibrosis has not been established. More research is needed.

Texture analysis of liver parenchyma to diagnose liver cirrhosis has been performed using contrast media. After injection of superparamagnetic iron oxides (SPIOs) or gadolinium chelates, hyperintense reticulations, which are postulated to represent septal fibrosis, can be observed in cirrhotic liver. It is known that SPIOs accumulate within liver reticuloendothelial cells after intravenous infusion, causing T2* shortening and reducing liver signal intensity. In cirrhotic liver, SPIOs accumulate and cause T2* shortening of normal liver parenchyma. Fibrosis appears in a hyperintense reticular pattern on T2 or T2* images. In addition, delayed T1 shortening and delayed enhancement of the hepatic fibrosis signal intensity by gadolinium chelates is expected (Figure 7). A double-contrast material-enhanced MRI protocol with sequential administration of SPIOs and gadolinium chelates was superior to a single-contrast material-enhanced MRI protocol for liver fibrosis diagnosis^[57]. However, these

protocols are no longer popular.

Gadoxetate disodium is a liver-specific MRI contrast agent with combined perfusion and hepatocyte-selective properties. Hepatocyte-phase gadoxetate disodium-enhanced MRI can be used to measure hepatocyte function^[58-60]. One study shows that the contrast enhancement index (CEI = signal intensity post-enhancement/signal intensity pre-enhancement) in gadoxetate disodium-enhanced MRI more accurately correlated with hepatic fibrosis staging than ADC values (CEI: $r = -0.79$, ADC: $r = -0.43$)^[61]. Another study shows that heterogeneity of hepatic parenchyma enhancement on Hepatocyte-phase gadoxetate disodium-enhanced MRI is correlated with the degree of liver parenchyma fibrosis using parameter of corrected coefficient of variation [$CV = (SD_{liver} - SD_{air})/SI_{liver} \times 100$] (Figure 8)^[62].

CONCLUSION

The development of new imaging modalities for diagnosing of liver cirrhosis has led to the detection and measurement of subtle changes. This has enabled early and accurate diagnosis of liver cirrhosis. Currently, elastography, used to measure the stiffness and elasticity of

the liver, is more widely applied than texture analysis in diagnosis of liver cirrhosis. Results strongly correlate with hepatic fibrosis, without the need for a post-operation procedure. Although MRE has more accurate tendency, US is simple imaging tool in diagnosing cirrhosis and can be added as several additional complementary technologies. The non-inferior diagnostic capability, non-invasiveness and relative cost-effectiveness of US elastography may enable it to be one of the most useful techniques for diagnosis of liver cirrhosis.

We expect standardization of elastography techniques so that quantitative parameters obtained by clinical systems from different vendors may give similar results in the future.

REFERENCES

- 1 **Massarrat S**, Fallahzad V, Kamalian N. Clinical, biochemical and imaging-verified regression of hepatitis B-induced cirrhosis. *Liver Int* 2004; **24**: 105-109 [PMID: 15078473 DOI: 10.1111/j.1478-3231.2004.00895.x]
- 2 **Ghany MG**, Strader DB, Thomas DL, Seeff LB. Diagnosis, management, and treatment of hepatitis C: an update. *Hepatology* 2009; **49**: 1335-1374 [PMID: 19330875 DOI: 10.1002/hep.22759]
- 3 **Castera L**. Invasive and non-invasive methods for the assessment of fibrosis and disease progression in chronic liver disease. *Best Pract Res Clin Gastroenterol* 2011; **25**: 291-303 [PMID: 21497746 DOI: 10.1016/j.bpg.2011.02.003]
- 4 **Ishak K**, Baptista A, Bianchi L, Callea F, De Groote J, Gudat F, Denk H, Desmet V, Korb G, MacSween RN. Histological grading and staging of chronic hepatitis. *J Hepatol* 1995; **22**: 696-699 [PMID: 7560864]
- 5 **Maharaj B**, Maharaj RJ, Leary WP, Cooppan RM, Naran AD, Pirie D, Pudifin DJ. Sampling variability and its influence on the diagnostic yield of percutaneous needle biopsy of the liver. *Lancet* 1986; **1**: 523-525 [PMID: 2869260]
- 6 **Seeff LB**, Everson GT, Morgan TR, Curto TM, Lee WM, Ghany MG, Shiffman ML, Fontana RJ, Di Bisceglie AM, Bonkovsky HL, Dienstag JL. Complication rate of percutaneous liver biopsies among persons with advanced chronic liver disease in the HALT-C trial. *Clin Gastroenterol Hepatol* 2010; **8**: 877-883 [PMID: 20362695 DOI: 10.1016/j.cgh.2010.03.025]
- 7 **Bravo AA**, Sheth SG, Chopra S. Liver biopsy. *N Engl J Med* 2001; **344**: 495-500 [PMID: 11172192 DOI: 10.1056/nejm200102153440706]
- 8 **Parkes J**, Guha IN, Roderick P, Rosenberg W. Performance of serum marker panels for liver fibrosis in chronic hepatitis C. *J Hepatol* 2006; **44**: 462-474 [PMID: 16427156 DOI: 10.1016/j.jhep.2005.10.019]
- 9 **Grigorescu M**. Noninvasive biochemical markers of liver fibrosis. *J Gastrointest Liver Dis* 2006; **15**: 149-159 [PMID: 16802010]
- 10 **Zardi EM**, Caturelli E. May sonography distinguish between liver fibrosis and liver steatosis? *Dig Liver Dis* 2007; **39**: 790 [PMID: 17604239 DOI: 10.1016/j.dld.2007.05.001]
- 11 **Colli A**, Fraquelli M, Andreoletti M, Marino B, Zuccoli E, Conte D. Severe liver fibrosis or cirrhosis: accuracy of US for detection-analysis of 300 cases. *Radiology* 2003; **227**: 89-94 [PMID: 12601199 DOI: 10.1148/radiol.2272020193]
- 12 **Viganò M**, Visentin S, Aghemo A, Rumi MG, Ronchi G. US features of liver surface nodularity as a predictor of severe fibrosis in chronic hepatitis C. *Radiology* 2005; **234**: 641; author reply 641 [PMID: 15671013 DOI: 10.1148/radiol.2342041267]
- 13 **Soresi M**, Giannitrapani L, Cervello M, Licata A, Montalto G. Non invasive tools for the diagnosis of liver cirrhosis. *World J Gastroenterol* 2014; **20**: 18131-18150 [PMID: 25561782 DOI: 10.3748/wjg.v20.i48.18131]
- 14 **Hartman PC**, Oosterveld BJ, Thijssen JM, Rosenbusch GJ, van den Berg J. Detection and differentiation of diffuse liver disease by quantitative echography. A retrospective assessment. *Invest Radiol* 1993; **28**: 1-6 [PMID: 8425846]
- 15 **Layer G**, Zuna I, Lorenz A, Zerban H, Haberkorn U, Bannasch P, van Kaick G, Räh U. Computerized ultrasound B-scan texture analysis of experimental diffuse parenchymal liver disease: correlation with histopathology and tissue composition. *J Clin Ultrasound* 1991; **19**: 193-201 [PMID: 1646222]
- 16 **Lee CH**, Choi JW, Kim KA, Seo TS, Lee JM, Park CM. Usefulness of standard deviation on the histogram of ultrasound as a quantitative value for hepatic parenchymal echo texture; preliminary study. *Ultrasound Med Biol* 2006; **32**: 1817-1826 [PMID: 17169693 DOI: 10.1016/j.ultrasmedbio.2006.06.014]
- 17 **Li R**, Hua X, Guo Y, Zhang P, Guo A. Neighborhood-pixels algorithm combined with Sono-CT in the diagnosis of cirrhosis: an experimental study. *Ultrasound Med Biol* 2006; **32**: 1515-1520 [PMID: 17045872 DOI: 10.1016/j.ultrasmedbio.2006.06.009]
- 18 **Vicas C**, Lupsor M, Socaciu M, Nedevschi S, Badea R. Influence of expert-dependent variability over the performance of non-invasive fibrosis assessment in patients with chronic hepatitis C by means of texture analysis. *Comput Math Methods Med* 2012; **2012**: 346713 [PMID: 22229041 DOI: 10.1155/2012/346713]
- 19 **K C S**, Sharma D, Chataut SP. Hepatic vein waveforms in liver cirrhosis re-evaluated. *Hepatol Int* 2010; **5**: 581-585 [PMID: 21442056 DOI: 10.1007/s12072-010-9226-y]
- 20 **Kok T**, van der Jagt EJ, Haagsma EB, Bijleveld CM, Jansen PL, Boeve WJ. The value of Doppler ultrasound in cirrhosis and portal hypertension. *Scand J Gastroenterol Suppl* 1999; **230**: 82-88 [PMID: 10499467]
- 21 **Yin XY**, Lu MD, Huang JF, Xie XY, Liang LJ. Color Doppler velocity profile assessment of portal hemodynamics in cirrhotic patients with portal hypertension: correlation with esophageal variceal bleeding. *J Clin Ultrasound* 2001; **29**: 7-13 [PMID: 11180179]
- 22 **Bernatik T**, Strobel D, Hahn EG, Becker D. Doppler measurements: a surrogate marker of liver fibrosis? *Eur J Gastroenterol Hepatol* 2002; **14**: 383-387 [PMID: 11943950]
- 23 **Tang A**, Kim TK, Heathcote J, Guindi M, Jang HJ, Karshafian R, Burns PN, Wilson SR. Does hepatic vein transit time performed with contrast-enhanced ultrasound predict the severity of hepatic fibrosis? *Ultrasound Med Biol* 2011; **37**: 1963-1969 [PMID: 22033130 DOI: 10.1016/j.ultrasmedbio.2011.09.010]
- 24 **Lim AK**, Taylor-Robinson SD, Patel N, Eckersley RJ, Goldin RD, Hamilton G, Foster GR, Thomas HC, Cosgrove DO, Blomley MJ. Hepatic vein transit times using a microbubble agent can predict disease severity non-invasively in patients with hepatitis C. *Gut* 2005; **54**: 128-133 [PMID: 15591518 DOI: 10.1136/gut.2003.030965]
- 25 **Sandrin L**, Fourquet B, Hasquenoh JM, Yon S, Fournier C, Mal F, Christidis C, Zioli M, Poulet B, Kazemi F, Beaugrand M, Palau R. Transient elastography: a new noninvasive method for assessment of hepatic fibrosis. *Ultrasound Med Biol* 2003; **29**: 1705-1713 [PMID: 14698338]
- 26 **Friedrich-Rust M**, Ong MF, Martens S, Sarrazin C, Bojunga J, Zeuzem S, Herrmann E. Performance of transient elastography for the staging of liver fibrosis: A meta-analysis. *Gastroenterology* 2008; **134**: 960-974 [DOI: 10.1053/j.gastro.2008.01.034]
- 27 **Sporea I**, Sirlu R, Deleanu A, Tudora A, Popescu A, Curescu M, Bota S. Liver stiffness measurements in patients with HBV vs HCV chronic hepatitis: a comparative study. *World J Gastroenterol* 2010; **16**: 4832-4837 [PMID: 20939112 DOI: 10.3748/wjg.v16.i38.4832]
- 28 **Riggio S**, Mamone F, Mandraffino G, Maimone S, Alibrandi A, Manti L, Saitta C, Tripodi PF, Sardo MA, Squadrito G, Saitta A. Assessment of liver stiffness in subjects affected by familial combined hyperlipidaemia with hepatic steatosis. *Eur J Clin Invest* 2010; **40**: 722-728 [PMID: 20561029 DOI: 10.1111/j.1365-2362.2010.02323.x]
- 29 **Chon YE**, Choi EH, Song KJ, Park JY, Kim do Y, Han KH, Chon CY, Ahn SH, Kim SU. Performance of transient elastography for the staging of liver fibrosis in patients with chronic hepatitis B: a

- meta-analysis. *PLoS One* 2012; **7**: e44930 [PMID: 23049764 DOI: 10.1371/journal.pone.0044930]
- 30 **Castéra L**, Foucher J, Bernard PH, Carvalho F, Allaix D, Merrouche W, Couzigou P, de Lédinghen V. Pitfalls of liver stiffness measurement: a 5-year prospective study of 13,369 examinations. *Hepatology* 2010; **51**: 828-835 [PMID: 20063276 DOI: 10.1002/hep.23425]
- 31 **Yap WW**, Kirke R, Yoshida EM, Owen D, Harris AC. Non-invasive assessment of liver fibrosis using ARFI with pathological correlation, a prospective study. *Ann Hepatol* 2013; **12**: 608-615 [PMID: 23813139]
- 32 **Bota S**, Herkner H, Sporea I, Salzl P, Sirlu R, Neghina AM, Peck-Radosavljevic M. Meta-analysis: ARFI elastography versus transient elastography for the evaluation of liver fibrosis. *Liver Int* 2013; **33**: 1138-1147 [PMID: 23859217 DOI: 10.1111/liv.12240]
- 33 **Tada T**, Kumada T, Toyoda H, Ito T, Sone Y, Okuda S, Tsuji N, Imayoshi Y, Yasuda E. Utility of real-time shear wave elastography for assessing liver fibrosis in patients with chronic hepatitis C infection without cirrhosis: Comparison of liver fibrosis indices. *Hepatol Res* 2015; Epub ahead of print [PMID: 25580959 DOI: 10.1111/hepr.12476]
- 34 **Samir AE**, Dhyani M, Vij A, Bhan AK, Halpern EF, Méndez-Navarro J, Corey KE, Chung RT. Shear-wave elastography for the estimation of liver fibrosis in chronic liver disease: determining accuracy and ideal site for measurement. *Radiology* 2015; **274**: 888-896 [PMID: 25393946 DOI: 10.1148/radiol.14140839]
- 35 **Yoon JH**, Lee JM, Han JK, Choi BI. Shear wave elastography for liver stiffness measurement in clinical sonographic examinations: evaluation of intraobserver reproducibility, technical failure, and unreliable stiffness measurements. *J Ultrasound Med* 2014; **33**: 437-447 [PMID: 24567455 DOI: 10.7863/ultra.33.3.437]
- 36 **Tutar O**, Beşer ÖF, Adaletli I, Tunc N, Gulcu D, Kantarci F, Mihmanli I, Cokugras FC, Kutlu T, Ozbay G, Erkan T. Shear wave elastography in the evaluation of liver fibrosis in children. *J Pediatr Gastroenterol Nutr* 2014; **58**: 750-755 [PMID: 24552673 DOI: 10.1097/MPG.0000000000000329]
- 37 **Cassinotto C**, Lapuyade B, Mouries A, Hiriart JB, Vergniol J, Gaye D, Castain C, Le Bail B, Chermak F, Foucher J, Laurent F, Montaudon M, De Ledinghen V. Non-invasive assessment of liver fibrosis with impulse elastography: comparison of Supersonic Shear Imaging with ARFI and FibroScan®. *J Hepatol* 2014; **61**: 550-557 [PMID: 24815876 DOI: 10.1016/j.jhep.2014.04.044]
- 38 **Kudo M**, Zheng RQ, Kim SR, Okabe Y, Osaki Y, Iijima H, Itani T, Kasugai H, Kanematsu M, Ito K, Usuki N, Shimamatsu K, Kage M, Kojiro M. Diagnostic accuracy of imaging for liver cirrhosis compared to histologically proven liver cirrhosis. A multicenter collaborative study. *Intervirology* 2008; **51** Suppl 1: 17-26 [PMID: 18544944 DOI: 10.1159/000122595]
- 39 **Varenika V**, Fu Y, Maher JJ, Gao D, Kakar S, Cabarrus MC, Yeh BM. Hepatic fibrosis: evaluation with semiquantitative contrast-enhanced CT. *Radiology* 2013; **266**: 151-158 [PMID: 23169796 DOI: 10.1148/radiol.12112452]
- 40 **Gülberg V**, Haag K, Rössle M, Gerbes AL. Hepatic arterial buffer response in patients with advanced cirrhosis. *Hepatology* 2002; **35**: 630-634 [PMID: 11870377 DOI: 10.1053/jhep.2002.31722]
- 41 **Hashimoto K**, Murakami T, Dono K, Hori M, Kim T, Kudo M, Marubashi S, Miyamoto A, Takeda Y, Nagano H, Umeshita K, Nakamura H, Monden M. Assessment of the severity of liver disease and fibrotic change: the usefulness of hepatic CT perfusion imaging. *Oncol Rep* 2006; **16**: 677-683 [PMID: 16969479]
- 42 **Miles KA**, Hayball MP, Dixon AK. Functional images of hepatic perfusion obtained with dynamic CT. *Radiology* 1993; **188**: 405-411 [PMID: 8327686 DOI: 10.1148/radiology.188.2.8327686]
- 43 **Ronot M**, Asselah T, Paradis V, Michoux N, Dorvillius M, Baron G, Marcellin P, Van Beers BE, Vilgrain V. Liver fibrosis in chronic hepatitis C virus infection: differentiating minimal from intermediate fibrosis with perfusion CT. *Radiology* 2010; **256**: 135-142 [PMID: 20574090 DOI: 10.1148/radiol.10091295]
- 44 **Faria SC**, Ganesan K, Mwangi I, Shiehorteza M, Viamonte B, Mazhar S, Peterson M, Kono Y, Santillan C, Casola G, Sirlin CB. MR imaging of liver fibrosis: Current state of the art. *RSNA* 2009; **29**: 1615-1635 [DOI: 10.1148/rg.296095512]
- 45 **Annet L**, Peeters F, Abarca-Quinones J, Leclercq I, Moulin P, Van Beers BE. Assessment of diffusion-weighted MR imaging in liver fibrosis. *J Magn Reson Imaging* 2007; **25**: 122-128 [PMID: 17154179 DOI: 10.1002/jmri.20771]
- 46 **Bakan AA**, Inci E, Bakan S, Gokturk S, Cimilli T. Utility of diffusion-weighted imaging in the evaluation of liver fibrosis. *Eur Radiol* 2012; **22**: 682-687 [PMID: 21984447 DOI: 10.1007/s00330-011-2295-z]
- 47 **Sandrasegaran K**, Akisik FM, Lin C, Tahir B, Rajan J, Saxena R, Aisen AM. Value of diffusion-weighted MRI for assessing liver fibrosis and cirrhosis. *AJR Am J Roentgenol* 2009; **193**: 1556-1560 [PMID: 19933647 DOI: 10.2214/ajr.09.2436]
- 48 **Le Bihan D**, Breton E, Lallemand D, Aubin ML, Vignaud J, Laval-Jeantet M. Separation of diffusion and perfusion in intravoxel incoherent motion MR imaging. *Radiology* 1988; **168**: 497-505 [PMID: 3393671 DOI: 10.1148/radiology.168.2.3393671]
- 49 **Luciani A**, Vignaud A, Cavet M, Nhieu JT, Mallat A, Ruel L, Laurent A, Deux JF, Brugieres P, Rahmouni A. Liver cirrhosis: intravoxel incoherent motion MR imaging--pilot study. *Radiology* 2008; **249**: 891-899 [PMID: 19011186 DOI: 10.1148/radiol.2493080080]
- 50 **Yoon JH**, Lee JM, Baek JH, Shin CI, Kiefer B, Han JK, Choi BI. Evaluation of hepatic fibrosis using intravoxel incoherent motion in diffusion-weighted liver MRI. *J Comput Assist Tomogr* 2014; **38**: 110-116 [PMID: 24378888 DOI: 10.1097/RCT.0b013e3182a589be]
- 51 **Wang Y**, Ganger DR, Levitsky J, Sternick LA, McCarthy RJ, Chen ZE, Fasanati CW, Bolster B, Shah S, Zuehlsdorff S, Omary RA, Ehman RL, Miller FH. Assessment of chronic hepatitis and fibrosis: comparison of MR elastography and diffusion-weighted imaging. *AJR Am J Roentgenol* 2011; **196**: 553-561 [PMID: 21343496 DOI: 10.2214/ajr.10.4580]
- 52 **Yin M**, Talwalkar JA, Glaser KJ, Manduca A, Grimm RC, Rossman PJ, Fidler JL, Ehman RL. Assessment of hepatic fibrosis with magnetic resonance elastography. *Clin Gastroenterol Hepatol* 2007; **5**: 1207-1213.e2 [PMID: 17916548 DOI: 10.1016/j.cgh.2007.06.012]
- 53 **Zou LQ**, Chen J, Pan L, Jiang JZ, Xing W. Comparison of magnetic resonance elastography and diffusion-weighted imaging for staging hepatic fibrosis. *Chin Med J (Engl)* 2015; **128**: 620-625 [PMID: 25698193 DOI: 10.4103/0366-6999.151659]
- 54 **Rustogi R**, Horowitz J, Harmath C, Wang Y, Chalian H, Ganger DR, Chen ZE, Bolster BD, Shah S, Miller FH. Accuracy of MR elastography and anatomic MR imaging features in the diagnosis of severe hepatic fibrosis and cirrhosis. *J Magn Reson Imaging* 2012; **35**: 1356-1364 [PMID: 22246952 DOI: 10.1002/jmri.23585]
- 55 **Chamarthi SK**, Raterman B, Mazumder R, Michaels A, Oza VM, Hanje J, Bolster B, Jin N, White RD, Kolipaka A. Rapid acquisition technique for MR elastography of the liver. *Magn Reson Imaging* 2014; **32**: 679-683 [PMID: 24637083 DOI: 10.1016/j.mri.2014.02.013]
- 56 **Yoon JH**, Lee JM, Joo I, Lee ES, Sohn JY, Jang SK, Lee KB, Han JK, Choi BI. Hepatic fibrosis: prospective comparison of MR elastography and US shear-wave elastography for evaluation. *Radiology* 2014; **273**: 772-782 [PMID: 25007047 DOI: 10.1148/radiol.14132000]
- 57 **Aguirre DA**, Behling CA, Alpert E, Hassanein TI, Sirlin CB. Liver fibrosis: noninvasive diagnosis with double contrast material-enhanced MR imaging. *Radiology* 2006; **239**: 425-437 [PMID: 16641352 DOI: 10.1148/radiol.2392050505]
- 58 **Nilsson H**, Nordell A, Vargas R, Douglas L, Jonas E, Blomqvist L. Assessment of hepatic extraction fraction and input relative blood flow using dynamic hepatocyte-specific contrast-enhanced MRI. *J Magn Reson Imaging* 2009; **29**: 1323-1331 [PMID: 19472389 DOI: 10.1002/jmri.21801]
- 59 **Ryeom HK**, Kim SH, Kim JY, Kim HJ, Lee JM, Chang YM, Kim YS, Kang DS. Quantitative evaluation of liver function with MRI Using Gd-EOB-DTPA. *Korean J Radiol* 2004; **5**: 231-239 [PMID: 15637473]
- 60 **Shimizu J**, Dono K, Gotoh M, Hasuie Y, Kim T, Murakami T,

- Sakon M, Umeshita K, Nagano H, Nakamori S, Kato N, Miyazawa T, Nakamura H, Monden M. Evaluation of regional liver function by gadolinium-EOB-DTPA-enhanced MR imaging. *Dig Dis Sci* 1999; **44**: 1330-1337 [PMID: 10489914]
- 61 **Watanabe H**, Kanematsu M, Goshima S, Kondo H, Onozuka M, Moriyama N, Bae KT. Staging hepatic fibrosis: comparison of gadoxetate disodium-enhanced and diffusion-weighted MR imaging--preliminary observations. *Radiology* 2011; **259**: 142-150 [PMID: 21248234 DOI: 10.1148/radiol.10100621]
- 62 **Kim H**, Park SH, Kim EK, Kim MJ, Park YN, Park HJ, Choi JY. Histogram analysis of gadoxetic acid-enhanced MRI for quantitative hepatic fibrosis measurement. *PLoS One* 2014; **9**: e114224 [PMID: 25460180 DOI: 10.1371/journal.pone.0114224]
- 63 **Deffieux T**, Gennisson JL, Bousquet L, Corouge M, Cosconea S, Amroun D, Tripon S, Terris B, Mallet V, Sogni P, Tanter M, Pol S. Investigating liver stiffness and viscosity for fibrosis, steatosis and activity staging using shear wave elastography. *J Hepatol* 2015; **62**: 317-324 [PMID: 25251998 DOI: 10.1016/j.jhep.2014.09.020]
- 64 **Jeong JY**, Kim TY, Sohn JH, Kim Y, Jeong WK, Oh YH, Yoo KS. Real time shear wave elastography in chronic liver diseases: accuracy for predicting liver fibrosis, in comparison with serum markers. *World J Gastroenterol* 2014; **20**: 13920-13929 [PMID: 25320528 DOI: 10.3748/wjg.v20.i38.13920]
- 65 **Ferraioli G**, Parekh P, Levitov AB, Filice C. Shear wave elastography for evaluation of liver fibrosis. *J Ultrasound Med* 2014; **33**: 197-203 [PMID: 24449721 DOI: 10.7863/ultra.33.2.197]
- 66 **Singh S**, Venkatesh SK, Wang Z, Miller FH, Motosugi U, Low RN, Hassanein T, Asbach P, Godfrey EM, Yin M, Chen J, Keaveny AP, Bridges M, Bohte A, Murad MH, Lomas DJ, Talwalkar JA, Ehman RL. Diagnostic performance of magnetic resonance elastography in staging liver fibrosis: a systematic review and meta-analysis of individual participant data. *Clin Gastroenterol Hepatol* 2015; **13**: 440-451.e6 [PMID: 25305349 DOI: 10.1016/j.cgh.2014.09.046]
- 67 **Venkatesh SK**, Yin M, Takahashi N, Glockner JF, Talwalkar JA, Ehman RL. Non-invasive detection of liver fibrosis: MR imaging features vs. MR elastography. *Abdom Imaging* 2015; **40**: 766-775 [PMID: 25805619 DOI: 10.1007/s00261-015-0347-6]
- 68 **Venkatesh SK**, Wang G, Lim SG, Wee A. Magnetic resonance elastography for the detection and staging of liver fibrosis in chronic hepatitis B. *Eur Radiol* 2014; **24**: 70-78 [PMID: 23928932 DOI: 10.1007/s00330-013-2978-8]
- 69 **Shi Y**, Guo Q, Xia F, Dzyubak B, Glaser KJ, Li Q, Li J, Ehman RL. MR elastography for the assessment of hepatic fibrosis in patients with chronic hepatitis B infection: does histologic necroinflammation influence the measurement of hepatic stiffness? *Radiology* 2014; **273**: 88-98 [PMID: 24893048 DOI: 10.1148/radiol.14132592]
- 70 **Loomba R**, Wolfson T, Ang B, Hooker J, Behling C, Peterson M, Valasek M, Lin G, Brenner D, Gamst A, Ehman R, Sirlin C. Magnetic resonance elastography predicts advanced fibrosis in patients with nonalcoholic fatty liver disease: a prospective study. *Hepatology* 2014; **60**: 1920-1928 [PMID: 25103310 DOI: 10.1002/hep.27362]
- 71 **Bohte AE**, de Niet A, Jansen L, Bipat S, Nederveen AJ, Verheij J, Terpstra V, Sinkus R, van Nieuwkerk KM, de Kneegt RJ, Baak BC, Jansen PL, Reesink HW, Stoker J. Non-invasive evaluation of liver fibrosis: a comparison of ultrasound-based transient elastography and MR elastography in patients with viral hepatitis B and C. *Eur Radiol* 2014; **24**: 638-648 [PMID: 24158528 DOI: 10.1007/s00330-013-3046-0]
- 72 **Kim D**, Kim WR, Talwalkar JA, Kim HJ, Ehman RL. Advanced fibrosis in nonalcoholic fatty liver disease: noninvasive assessment with MR elastography. *Radiology* 2013; **268**: 411-419 [PMID: 23564711 DOI: 10.1148/radiol.13121193]
- 73 **Wang QB**, Zhu H, Liu HL, Zhang B. Performance of magnetic resonance elastography and diffusion-weighted imaging for the staging of hepatic fibrosis: A meta-analysis. *Hepatology* 2012; **56**: 239-247 [PMID: 22278368 DOI: 10.1002/hep.25610]
- 74 **Kim BH**, Lee JM, Lee YJ, Lee KB, Suh KS, Han JK, Choi BI. MR elastography for noninvasive assessment of hepatic fibrosis: experience from a tertiary center in Asia. *J Magn Reson Imaging* 2011; **34**: 1110-1116 [PMID: 21932355 DOI: 10.1002/jmri.22723]

P- Reviewer: Song JS S- Editor: Song XX
L- Editor: A E- Editor: Liu SQ





Published by **Baishideng Publishing Group Inc**

8226 Regency Drive, Pleasanton, CA 94588, USA

Telephone: +1-925-223-8242

Fax: +1-925-223-8243

E-mail: bpgoffice@wjgnet.com

Help Desk: <http://www.wjgnet.com/esps/helpdesk.aspx>

<http://www.wjgnet.com>

